

DELFT UNIVERSITY OF TECHNOLOGY

SC42145 - ROBUST CONTROL

Control Design for a Floating Wind Turbine

November 27, 2020

Contents

1	Introduction	1
2	SISO controller design	2
2.1	Analysis of the plant characteristics	2
2.2	Controller synthesis	5
2.3	Closed-loop simulation	8
2.4	Disturbance rejection	11

1 Introduction

The goal of this report is to design a multi-input multi-output controller for an offshore floating wind turbine. Naturally, the motion of the sea causes a for-aft rocking motion of the wind-turbine which has to be controlled properly to avoid catastrophic damage to the plant. To do so, a linear state-space model has been derived to use as a basis for the controller synthesis.

In section 2 entails the design of a SISO that determines the blade pitch based on the generator speed.

2 SISO controller design

In this section, a SISO controller is designed connecting the first input and first output of the MIMO system, which are the blade pitch angle β and the generator speed ω_r . The primary concern is to keep the bandwidth of the system as high as possible while maintaining a very small overshoot and no steady-state error.

2.1 Analysis of the plant characteristics

The fifth-order transfer function of the plant is

$$G(s) = \frac{-0.07988s^4 - 0.003315s^3 - 0.8677s^2 + 0.006493s - 0.03458}{s^5 + 0.5979s^4 + 10.98s^3 + 4.709s^2 + 0.5421s + 0.1827} \quad (1)$$

The poles and zeros of the plant are visualized in fig. 1. Clearly, there are two slower complex pole pairs and one fast pole on the real axis.

In addition, there are two complex zero pairs close to the complex poles, one of which lies in the right-half plane. Hence, the system is nonminimum-phase, which will have substantial influence on the behaviour of the system and the controller synthesis. On the other hand, all the poles are in the left-half plane and the system is therefore open-loop stable, making it arguably easier to control. An overview of the poles of the system together with the corresponding damping ratio and time constants is given in table 1. The pole on the real axis is a lot faster than the two complex pairs; it will be of little importance for the controller design. The system has no pure integrators (i.e. poles in the origin) — it is therefore of

Table 1: Overview of the pole locations with the corresponding damping ratios, frequencies (specified in rad/s) and time constants. The fastest real pole is more than an order of magnitude faster than the slowest complex pair.

Pole location	Damping	Frequency	Time constant
$-0.0106 \pm 0.202i$	0.0522	0.203	94.6
-0.410	1.00	0.410	2.44
$-0.0832 \pm 3.29i$	0.0253	3.29	12.0

Type 0. These systems exhibit a finite steady-state error already for tracking a reference step. This is something that has to be taken care of in the controller design.

Some observations can be made from the Bode plot of the system shown in fig. 2. First of all, the steady-state gain of the system is *negative*, $-0.189\,29$ (450° corresponds to $\pm 180^\circ$). As such, a controller with negative (steady-state) gain will be required for tracking. The two dips in the body plot arise from the two complex pole and zero pairs that occur at very similar frequencies. These dips are the superposition of a resonance ‘dip’ and peak for both complex pairs.

The phase margin of the plant is infinite because the Bode plot never crosses the 0 dB line. Since the system is nonminimum phase, the gain margin is slightly easier read from

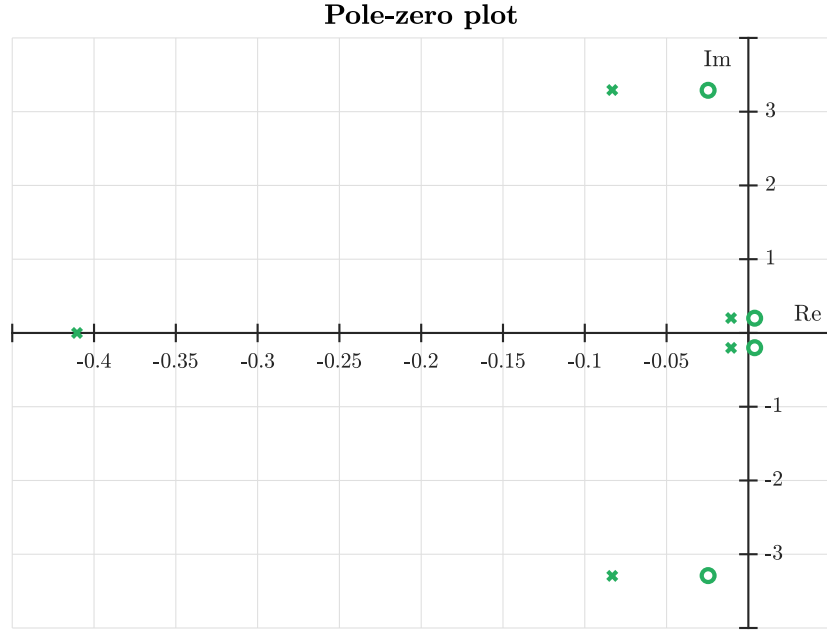


Figure 1: Pole-zero map of the plant transfer function as given by eq. (1).

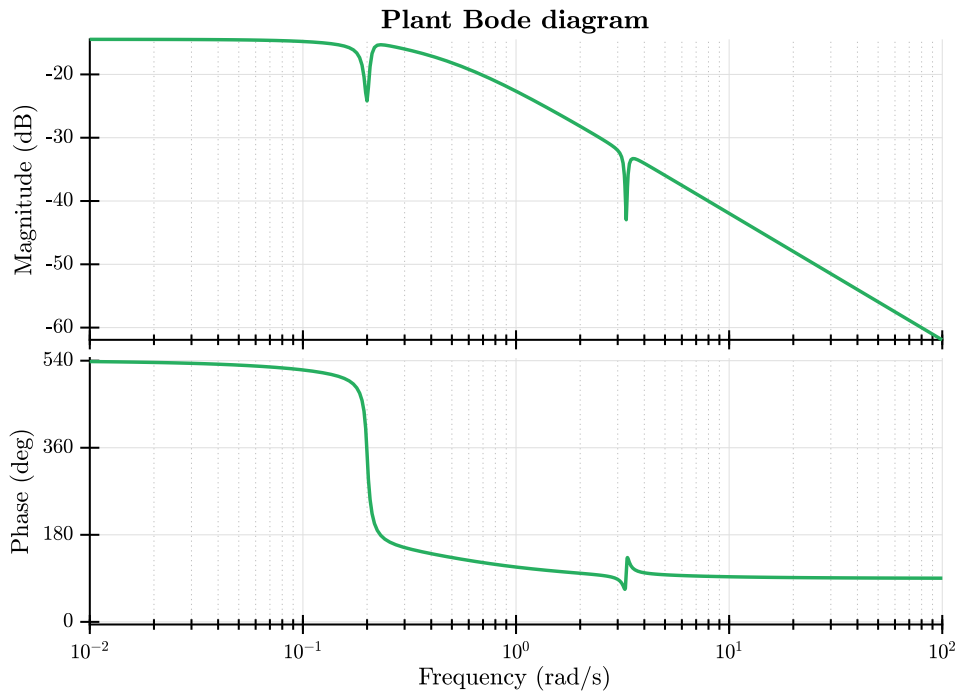


Figure 2: Bode plot of the plant transfer function.

the Nyquist diagram (fig. 3). It is important to note that this plot is given for the negative of the plant $-G(s)$ since the steady-state gain hints that a controller with negative gain will

be required — of course, the gain margin associated with positive gains is irrelevant. From the Nyquist plot the gain margin can be derived to be 24.2 dB at a frequency of 0.199 rad/s.

The right-half plane zeros impose a fundamental limit on the attainable bandwidth of the closed-loop system. This can be explained with the root locus: the right-half plane complex zero pair ‘attracts’ the complex pole pair. For sufficiently high gains, the closed-loop poles will enter the right-half plane as well, rendering the resulting system unstable. Hence, the fact that the system is nonminimum phase imposes inherent restrictions on the attainable bandwidth of the closed-loop system. [1]

An approximate quantitative limit on the crossover frequency of the loop transfer function (which in turn can be considered to be a reasonable approximation for the closed-loop system bandwidth) is provided by Skogestad and Postlethwaite [3] for complex right-half plane zero pairs $z = x \pm iy$:

$$\omega_B \approx \omega_c < \begin{cases} |z|/4 & \text{Re}(z) \gg \text{Im}(z) \\ |z|/2.8 & \text{Re}(z) = \text{Im}(z) \\ |z| & \text{Re}(z) \ll \text{Im}(z) \end{cases} \quad (2)$$

The right half plane zeros are a lot closer to the imaginary axis than they are to the real axis, which is why the latter case is most fit. As such, $\omega_B \approx \omega_c < 0.2 \text{ rad/s}$ or 0.0318 Hz .

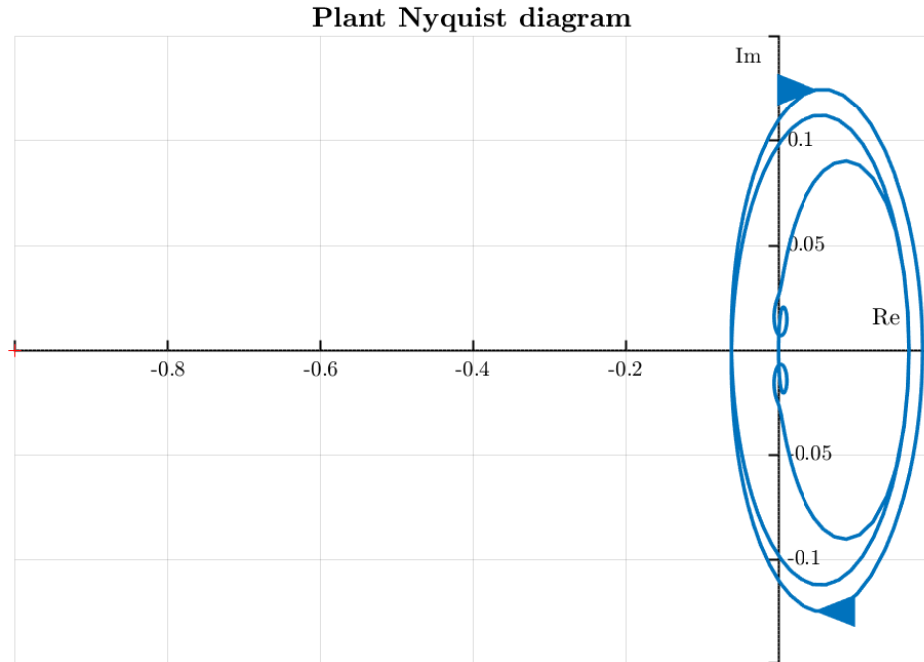


Figure 3: Nyquist plot of the plant.

2.2 Controller synthesis

For the controller synthesis we first select the most suitable controller by progressively adding control/compensation elements, assess their effects and combine them to meet a suitable controller structure which has the desired characteristics. The controller will then be tuned to meet the requirements.

The following frequency-response design requirements are based on a second-order approximation of the system and will be translated into requirements on the open loop bode diagram and complementary sensitivity function. Some iteration will be required to obtain the final results. [2]

- Overshoot $< 1\%$: A high phase margin for the open loop system is desired, since this is inversely related to the closed loop system overshoot. The damping ratio (ζ) that yields a specific overshoot is given by

$$\zeta = \frac{-\ln\left(\frac{PO}{100}\right)}{\sqrt{\pi^2 + \ln^2\left(\frac{PO}{100}\right)}}$$

which can be evaluated for the given percentage overshoot $PO = 1\%$. For a second-order approximation, this corresponds to a damping ratio of $\zeta \approx 0.83$. Subsequently, the damping ratio can be associated with a certain gain margin ϕ_M :

$$\phi_M = \tan^{-1} \frac{2\zeta}{\sqrt{-2\zeta^2 + \sqrt{1 + 4\zeta^4}}}$$

Hence, the phase margin should then approximately be 70.9 degrees.

- Small settling time: For a small settling time, the cross-over frequency should be as high as possible, since this directly affects the bandwidth frequency of the open loop system, which in turn is related to the settling time. The cross-over frequency can be increased by adding proportional gain.
- No steady-state error: to have zero steady-state error in a step response, the position constant K_p of the system must be infinity. Hence, $\lim_{s \rightarrow 0} L(s) = \infty$
- Stability and robustness: naturally sufficient gain and phase margin are required.

Since the requirements state that the settling time should be as small as possible, the goal is to create as much freedom as possible within the allowable design space, limited by the overshoot and steady-state requirements, in order to increase the bandwidth of the system as much as possible.

As mentioned before, the steady-state gain of the plant is negative, which is why negative feedback will be used to properly track the reference step. In fig. 4 the step responses are plotted for different proportional controllers. It is clear there is limited freedom to decrease the steady-state error and make the system response faster (because of the gain margin of

24.2 dB), so to remove the steady-state error integral action in the form of a PI controller is added.¹

Furthermore, observe the badly damped oscillatory artefacts in the step response. These oscillations are also clear from the root locus fig. 5, where the two imaginary pole pairs move closer towards the imaginary axis (and therefore with progressively lower damping constants), while maintaining roughly constant frequencies of 0.2 rad/s and 3.3 rad/s.

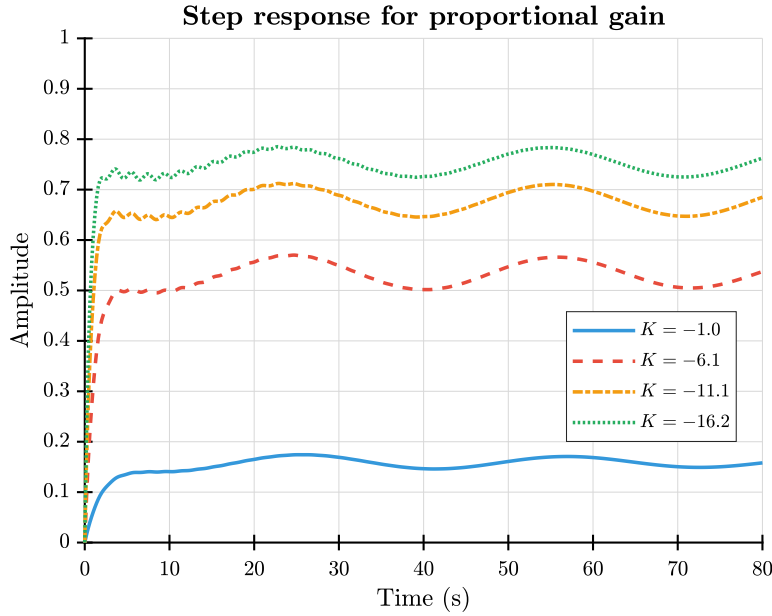


Figure 4: Step response for proportional gains. The case for $K = -16.2$ exactly corresponds to the gain margin; the corresponding oscillation does not decay over time.

The key design target for designing the integral term is to eliminate the steady-state error completely whilst minimizing the impact on the transient behaviour of the system. Since the system has infinite phase margin, this can be done without the immediate necessity of phase lead/D-action for stability. The initial settings for K_p and T_i are chosen based on the classical tuning rules for a PI controller of Ziegler and Nichols (1942). [3]

$$K_p = \frac{K_u}{2.2}, \quad T_i = \frac{P_u}{1.2}$$

with K_u the maximum controller gain and P_u the corresponding period of oscillations. So in our case

$$K_p = \frac{-16.21}{2.2} = -7.4 \quad T_i = \frac{1}{1.2} \frac{2\pi}{0.2 \text{ rad/s}} = 26.3$$

Keep in mind the Ziegler-Nichols provide suitable initial guesses, but the PI tuning values are somewhat aggressive and give a closed loop system with small stability margins and an

¹The presence of integral action is unavoidable, since the requirement of a zero steady-state gain cannot be obtained by just adding proportional gain or lag filters (infinite gain would be required).

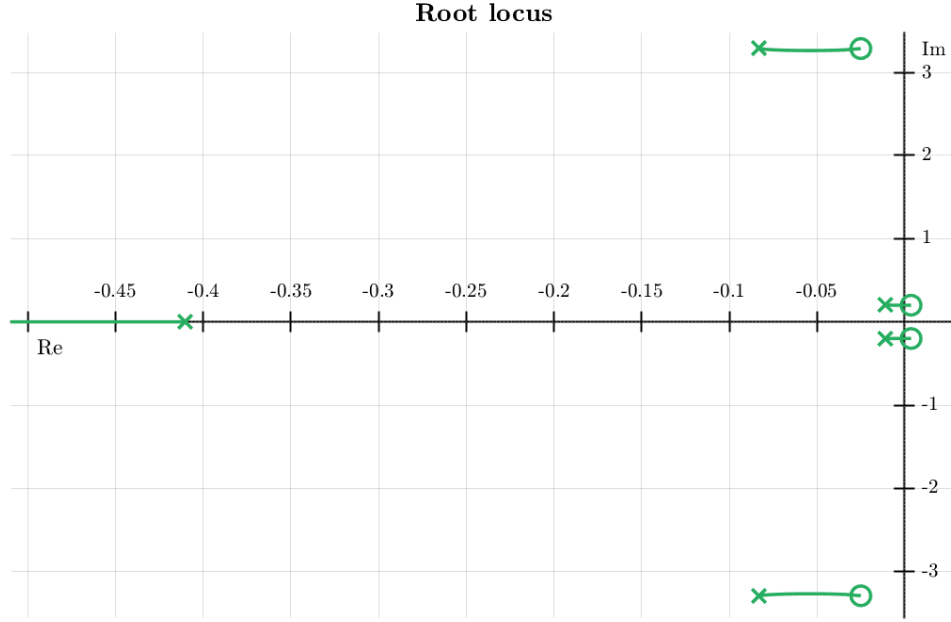


Figure 5: Root-locus plot of the plant for negative gain.

oscillating response. These characteristics will be removed by tuning the controller. Figure 6 shows the steady-state error is eliminated and the high frequency oscillations are significantly damped. However, the low frequency oscillations of the pole at 0.2 rad/s are not well-damped and clearly limit the performance of the controller.

Before tuning the PI controller, a second-order low-pass filter is added to suppress this frequency. A low-pass filter was chosen rather than adding derivative action to the PI controller, since the overshoot originates specifically from the oscillations induced by the pole at 0.2 rad/s, while the ‘overall’ system response is not too aggressive.

For the low-pass filter, the initial value for the cutoff frequency was set to $\omega_{\text{cut}} = 0.14$. For the damping ratio an initial value of $\beta = 0.7$ was chosen. The current controller structure will be suitable to start tuning the controller in order to meet our requirements (using MATLAB’s Control System Designer). The chosen controller design proved to be sufficient and resulted in the following transfer function.

$$K(s) = \frac{0.033052(s + 0.08554)}{s(s^2 + 0.2268s + 0.01309)} \quad (3)$$

Since a PI + low-pass controller has the following overall transfer function, the tuning parameters can be computed from the transfer function above. These tuning parameters can be found in table 2.

$$K(s) = \underbrace{\frac{\omega_n^2}{s^2 + 2\zeta\omega_n s + \omega_n^2}}_{\text{SO low-pass filter}} \underbrace{k_p \left(1 + \frac{1}{T_i s}\right)}_{\text{PI controller}}$$

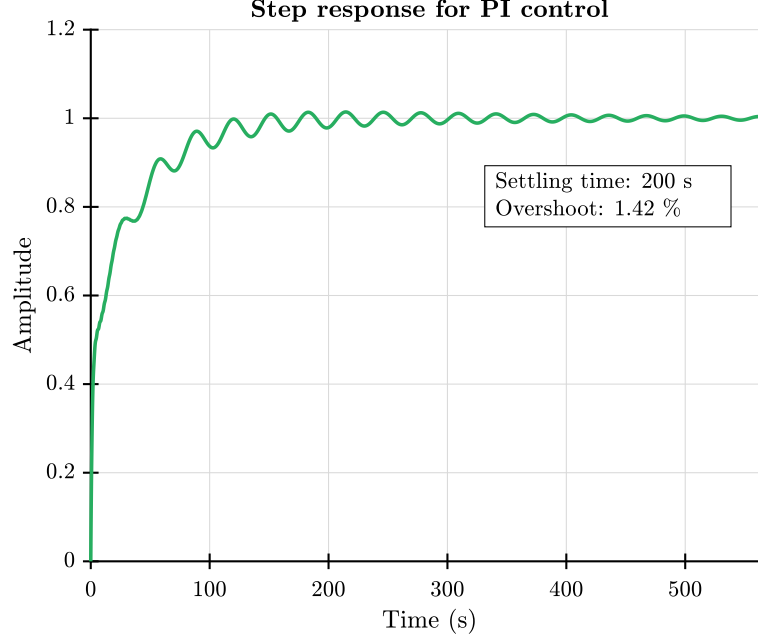


Figure 6: Step response of the plant controlled by a pure PI-controller. The undamped oscillations clearly cause a problem because they break the overshoot requirement while the bandwidth of the system is still relatively low.

Table 2: Tuning parameters of the final controller.

Parameter	Value
T_i	11.7
ω_n	0.114
ζ	0.991
k_p	-2.525

2.3 Closed-loop simulation

The performance of the designed controller for a reference response is shown in fig. 7. The associated time-domain characteristics are summarised in table 3. Clearly, the set performance requirements are satisfied. It has to be noted that the threshold for the settling time is defined to be 1 % (as opposed to 2 %, another common convention and the MATLAB default). The rationale behind this adjustment is that otherwise the settling time threshold would be higher than the allowable overshoot. One could possibly design a ‘faster’ controller (in terms of settling time) with an undershoot of more than 1 % (that is, after the initial overshoot the amplitude falls back below 99 % of the steady-state value) that technically meets the requirements. However, this approach was not taken since it would defeat the practical purpose of the imposed limits. Figure 8 depicts the associated controller effort

Table 3: Performance characteristics of the controlled system. All the requirements are satisfied and the gain and phase margin are adequate for robust performance.

Time-domain characteristics	
Rise time	32.3 s
Settling time	61.2 s
Overshoot	0.993 %
Peak time	71.0 s
Steady-state error	0
Frequency-domain characteristics	
Crossover frequency	0.040 rad/s
Bandwidth	0.065 rad/s
Phase margin	69.4°
Gain margin	16.4 dB

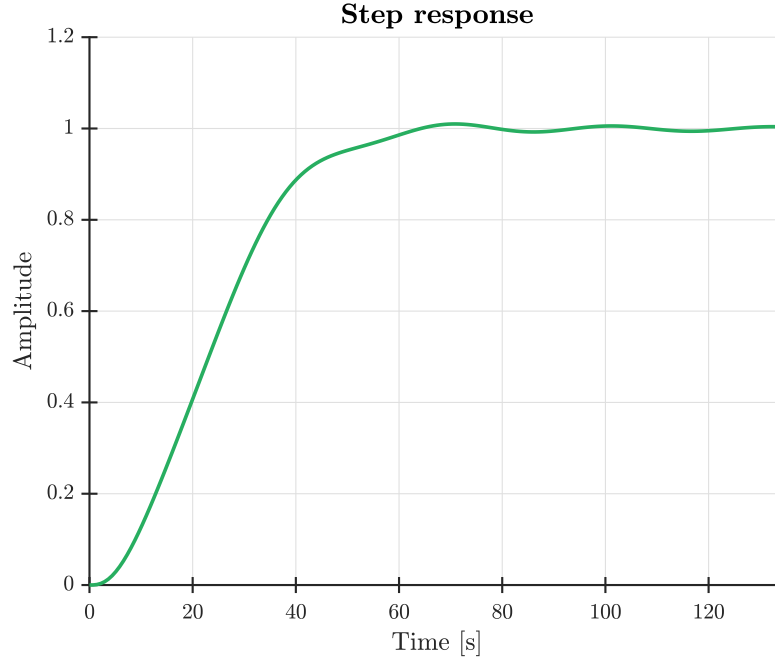


Figure 7: Step response of the closed-loop system with the tuned controller.

with the step response from fig. 7. As expected, the required control effort is negative.

Finally, the complementary sensitivity T of the closed-loop is shown in fig. 9. The bandwidth of the closed-loop system is $\omega_B = 0.065 \text{ rad/s} = 0.01 \text{ Hz}$, which is reasonably close to the limit imposed by the right-half plane zeros given by eq. (2). As is required for

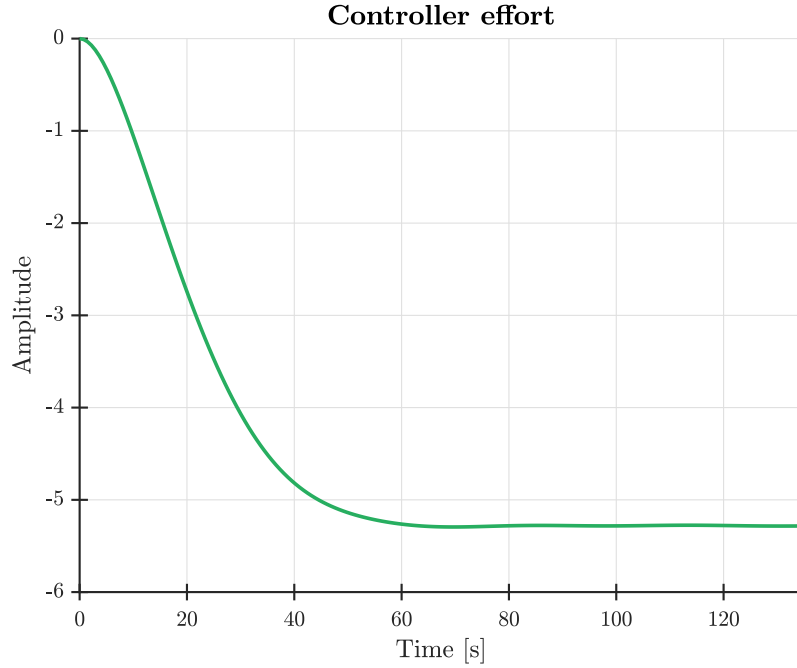


Figure 8: Controller effort corresponding with the step response in fig. 7.

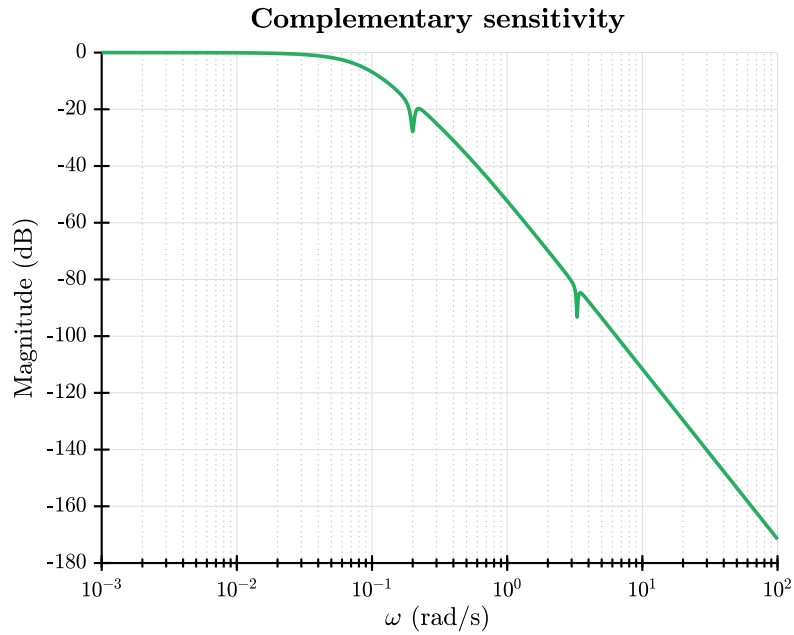


Figure 9: Complementary sensitivity T of the closed-loop.

zero steady-state error, $|T(0)| = 0$ dB.

Table 3 also shows some frequency-domain characteristics of the controlled system (beside the bandwidth). The phase and gain margins are ample for what is usually regarded as robust SISO performance.

2.4 Disturbance rejection

To investigate the disturbance rejection capabilities of the controller, a step input was simulated on the transfer function between the disturbance channel (the third input channel) and the output (generator speed). This corresponds to the following closed-loop transfer function:

$$G_{dr} = G_d(s)S(s)$$

with $G_d(s)$ being the open-loop transfer function between the disturbance and the output and $S(s) = \frac{1}{1+KG}$ the sensitivity of the closed-loop plant (including the controller).

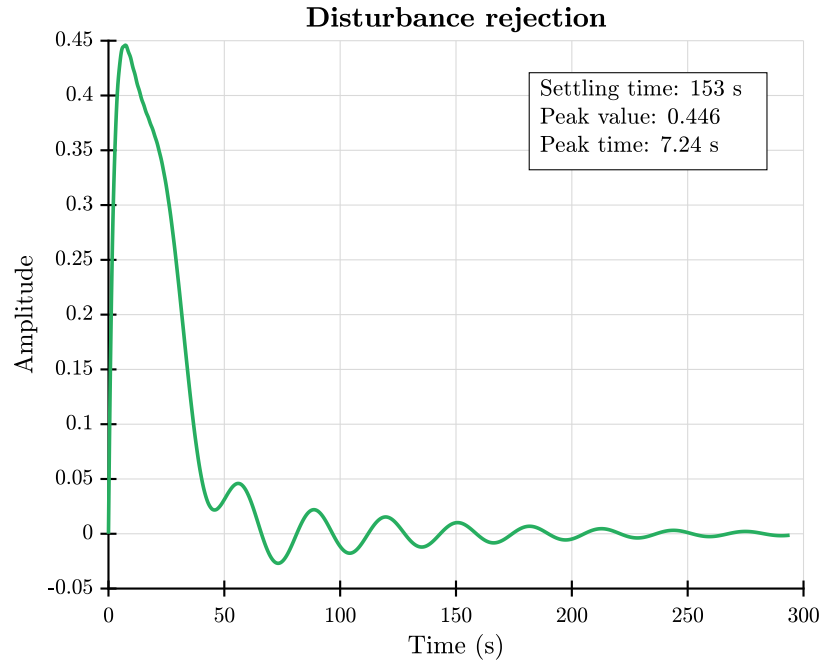


Figure 10: Reaction of the output on a disturbance step. Although the controller does the job, it certainly does not perform optimally in this regard.

The performance of the controller in this context is not as optimal as for the reference tracking scenario. First of all, the peak value is quite large, and there is a long period of decaying oscillations before the steady-state value of 0 is reached. Hence, some modifications are definitely in order if disturbance rejection would be a primary design objective for this controller.

References

- [1] R.H. Middleton. “Trade-offs in linear control system design”. In: *Automatica* 27.2 (1991), pp. 281–292. ISSN: 0005-1098. DOI: [https://doi.org/10.1016/0005-1098\(91\)90077-F](https://doi.org/10.1016/0005-1098(91)90077-F). URL: <http://www.sciencedirect.com/science/article/pii/000510989190077F>.
- [2] N.S. Nise. *Control Systems Engineering*. 6th ed. John Wiley and Sons, 2011.

- [3] S. Skogestad and I. Postlethwaite. *Multivariable Feedback Control - Analysis and Design*. 2nd ed. John Wiley and Sons, 2005.